



# All-aqueous emulsions stabilized by sporopollenin exine capsules

Diana Soto-Aguilar<sup>a</sup>, Elke Scholten<sup>b</sup>, Vincenzo Fogliano<sup>a</sup>, Ashkan Madadlou<sup>c,\*</sup>

<sup>a</sup> Food Quality and Design Group, Wageningen University, P.O. Box 17, 6700, AA, Wageningen, the Netherlands

<sup>b</sup> Physics and Physical Chemistry of Foods, Wageningen University, Bornse Weiland 9, 6708, WG, Wageningen, the Netherlands

<sup>c</sup> Department of Biotechnology and Food Science, Norwegian University of Science and Technology (NTNU), Trondheim, Norway

## ARTICLE INFO

### Keywords:

*Lycopodium clavatum*  
Capillary force  
Water-in-water emulsion

## ABSTRACT

The efficacy of sporopollenin exine capsules (SpECs) for stabilization of all-aqueous emulsions was assessed. Cytoplasmic substances were removed from *Lycopodium clavatum* spores to obtain the SpECs. SpECs had a comparable morphology with the parent spores, and a size of  $\sim 31 \mu\text{m}$ . The all-aqueous emulsions were prepared with polyethylene glycol (PEG) and dextran (Dex) at different PEG: Dex concentration ratios between 2:9 and 18:1. Confocal microscopy imaging showed that the emulsions were Dex-continuous at PEG: Dex concentration ratios of 2:9 and 4:8 and PEG-continuous at the ratios  $\geq 6:7$ . When the SpECs were initially suspended within the PEG phase, the Dex-continuous emulsions could not be stabilized. The SpECs also failed to stabilize the emulsion with a ratio of 6:7, where the emulsions transitioned to PEG-continuous. However, the SpECs could stabilize a bottom emulsion phase, consisting of Dex-rich droplets within the PEG exterior phase, at concentration ratios  $\geq 8:6$ . We hypothesized that a Pickering-type stabilization mechanism at the aqueous-aqueous interface of Dex droplets account for the emulsion stability, together with a possible formation of SpEC particle rafts. The emulsion stability at a concentration ratio of 8:6 was dependent on its pH; stable emulsions were formed at pH 7, but at pHs 2 and 4, the emulsions became unstable. These results were attributed to the high  $\zeta$ -potential ( $-31 \text{ mV}$ ) of the SpECs at pH 7. These results show that repulsion between dispersed droplets was more important than the packing of the particles at the interface itself.

## 1. Introduction

Functional and health-promoting foods are enthusiastically developed by researchers and industry. Such foods may contain bioactive ingredients like polyphenols, carotenoids, and bioactive peptides (Gonçalves, Martins, Duarte, Vicente, & Pinheiro, 2018; Li et al., 2022). The ingredients are however mostly chemically unstable, have low solubility in aqueous solutions, exert unpleasant tastes (Li et al., 2022; McClements, 2020), and are poorly digestible. Delivery systems such as oil-in-water emulsions and double emulsions can be used to protect the bioactive compounds against harsh conditions, increase their solubility in water, prevent their direct contact with in-mouth surfaces, and control their release in the gastrointestinal tract (Gonçalves et al., 2018; McClements, 2020). Nevertheless, oil-water emulsions have limitations, for instance, they contain a high-calorie oil phase and very commonly small (synthetic) surfactants (Li et al., 2022).

All-aqueous (water-in-water, W/W) emulsions are fat-free and surfactant-free systems that can be exploited for the encapsulation of water-soluble bioactive compounds (Troise, Fogliano, & Madadlou,

2020). They comprise two immiscible aqueous phases, each of which contains a (bio)polymer or salt (Madadlou, Saggiomo, Schroën, & Fogliano, 2020). Despite the environmental and consumer-associated advantages (i.e., absence of fat and synthetic surfactants) stabilization of all-aqueous emulsions remains a challenging task. The similar hydrophilicity of the two aqueous phases causes the interfacial tension between the phases to be extremely low ( $1 \mu\text{N/m}$ ). In addition, the interface consists of a diffuse aqueous layer, which is much thicker than oil-water interfaces (Scholten, Sagis, & Van Linden, 2006). Hence, small-molecule surfactants are unable to stabilize the water-water interface and prevent complete phase separation of the system (Esquena, 2016). Particles larger than the interfacial thickness are necessary to stabilize the water-water interface (Dickinson, 2019; Nicolai & Murray, 2017). The stabilization mechanism conferred by colloidal particles is commonly referred to as a Pickering mechanism. Non-organic colloidal particles such as latex and silica particles have been studied to stabilize all-aqueous emulsions (Dickinson, 2019). Also, some studies have used oil droplets, liposomes, cellulose nanocrystals, zein particles, and microbial cells for stabilization of all-aqueous

\* Corresponding author.

E-mail address: [Ashkan.madadlou@ntnu.no](mailto:Ashkan.madadlou@ntnu.no) (A. Madadlou).

<https://doi.org/10.1016/j.foodhyd.2023.109447>

Received 16 February 2023; Received in revised form 4 October 2023; Accepted 21 October 2023

Available online 22 October 2023

0268-005X/© 2023 The Authors. Published by Elsevier Ltd. This is an open access article under the CC BY license (<http://creativecommons.org/licenses/by/4.0/>).

emulsions (Chen et al., 2019; Dickinson, 2019; Hazt et al., 2020; Tea, Renou, & Nicolai, 2021). The hunt for food-grade Pickering particles (Nicolai & Murray, 2017), as well as other types of stabilizer particles is ongoing. In the present study, we take inspiration from nature at finding suitable particles for the stabilization of all-aqueous emulsions.

In addition, particles can self-organize via lateral capillary forces at the interface between two fluids of different densities (Protière, 2023). The floating structures at fluid-fluid interfaces are commonly referred to as "particle rafts" (Abkarian, Protière, Aristoff, & Stone, 2013; Protière, 2023).

Pollen and plant spores are particles filled with genetic material for reproduction purposes. They possess an inner cellulose layer (intine) which is surrounded by an outer sporopollenin layer (exine) covered by lipids (Diego-Taboada, Beckett, Atkin, & Mackenzie, 2014; Mikhael et al., 2020). Spores exhibit remarkable chemical and morphological stability attributed to their biological function of transporting and shielding the genetic material of plants for reproduction (Mackenzie, Boa, Diego-Taboada, Atkin, & Sathyapalan, 2015). Some constituents of the cytoplasm and the spore wall might trigger allergic responses (Bailey et al., 2019; Dahl, 2018), therefore they are often removed by chemical methods for food applications (Chiappe et al., 2020; Thomasson et al., 2020). After removing the surrounding fat layer and inner constituents of the spores, the resulting hollow particles are composed only of the exine layer, known as sporopollenin exine capsules (SpECs); they are hypoallergenic, non-toxic, and can be used as food ingredients (Bailey et al., 2019; Schouten et al., 2022).

The spore particles of *Lycopodium clavatum*, as well as the SpECs obtained from the *Lycopodium clavatum* spores have already been exploited as stabilizers in oil emulsification and liquid marble formation (Binks, Clint, Mackenzie, Simcock, & Whitby, 2005, 2011; Lagubeau, Rescaglio, & Melo, 2014). We hypothesized that the SpECs from *Lycopodium clavatum* can be likewise used as stabilizer particles in all-aqueous emulsions. The emulsions were prepared using one of the most well-known polymer-polymer pairs, i.e., dextran (Dex) and polyethylene glycol (PEG), which in aqueous environments segregatively phase-separate into all-aqueous emulsions (Madadlou et al., 2020). At the present study, initially SpECs were briefly characterized for shape, size and protein content. Then the SpECs usefulness for stabilization of all-aqueous emulsions was assessed, assuming that the particles can stabilize the interface by a Pickering-type mechanism, and form (loosely packed) rafts at the aqueous-aqueous interface. The findings may open a venue for the use of SpECs in food-grade systems.

## 2. Materials and methods

### 2.1. Materials

Spores from *Lycopodium clavatum* were purchased from Flame Water Circus (Sydney, Australia). PEG with an average molecular weight of 8 kDa, Dex with an average molecular weight of 500 kDa, fluorescently-labeled dextran, i.e., fluorescein isothiocyanate-dextran (500 kDa, FITC-Dex), and sodium azide were purchased from Sigma-Aldrich (Sigma-Aldrich, Co., Netherlands). Sodium hydroxide and hydrochloric acid were purchased from VWR International B.V. (Amsterdam, Netherlands). All other chemical reagents were of analytical grade and were used as received. De-ionized water from a Milli-Q system (Millipore, USA) was used for the preparation of all samples.

### 2.2. Extraction of sporopollenin exine capsules (SpECs)

SpECs were extracted from *Lycopodium clavatum* spores according to a protocol by Thomasson et al. (2020) with some modifications. Spores (50 g) were first defatted by suspending in acetone (300 mL) in a round-bottomed flask fitted with a glass condenser and heated at 60 °C for 3 h with gentle stirring. Then, spores were filtered under vacuum, washed with acetone (150 mL), and resuspended in new acetone (60 °C,

3 h). Afterward, spores were filtered, rinsed with acetone (300 mL) and ethanol (300 mL), and dried at 60 °C until a constant weight was obtained. For the extraction of SpECs, dry defatted spores were suspended in aqueous hydrochloric acid (9 M) in a round-bottomed flask fitted with a glass condenser and heated at 90 °C for 1 h with gentle stirring (Thomasson et al., 2020). The obtained SpECs were collected by filtration under vacuum and washed with Milli-Q water until neutral pH was obtained. Next, the SpECs were suspended in ethanol (to facilitate the drying process), stirred for 1 h, and collected by filtration under vacuum. Finally, SpECs were dried at 60 °C until constant weight and stored in the dark at 20 °C to remove any remaining ethanol and acetone from the SpECs.

### 2.3. Characterization of SpECs

#### 2.3.1. Particle size and $\zeta$ -potential

The average particle size of *Lycopodium* spores and SpECs was determined by static light scattering using a Mastersizer 2000 (Malvern Instruments Ltd., Worcestershire, UK) at 20 °C. The concentration of SpECs was 0.1 mg/mL, and the refractive indices of water and SpECs were set as 1.33 and 1.48, respectively (Barrier, 2008). Particle size is reported as D[3, 2].

The  $\zeta$ -potential of SpECs at different pH values was determined based on the electrophoretic mobility using an Ultra-Zetasizer Nano ZS (Malvern Instruments Ltd., Worcestershire, UK). The SpECs were dispersed in Milli-Q water at pH values of 2, 3, 4, 5, 6, and 7 (adjusted by HCl or NaOH 0.1 M). The dispersions were prepared either at 0.01 mg/mL (at pH 2) or 0.03 mg/mL (at pHs 3, 4, 5, 6, and 7), and were allowed to hydrate on a shaker (Heidolph, Multi Reax, Germany) for 8 h before  $\zeta$ -potential measurements were performed. The refractive and absorption indices of SpECs were set as 1.48 and 0.001, respectively (Barrier, 2008). The refractive index and dielectric constant of the dispersant (water) were taken as 1.330 and 80.4, respectively. The cell type used was DTS1070, and all measurements were carried out at least 2 times at 20 °C.

#### 2.3.2. Protein content and profile

The nitrogen content of *Lycopodium* spores and SpECs was determined by the Dumas combustion method using a Rapid N exceed nitrogen analyzer (Elementar, Langensfeld, Germany), following the manufacturer's protocol. A nitrogen conversion factor of 6.25 was used to convert measured nitrogen to protein content.

The protein profile of spores and SpECs was analyzed with sodium dodecyl sulfate-polyacrylamide gel electrophoresis (SDS-PAGE). Briefly, dry spores, defatted spores, and SpECs were fragmented using a cryomill (1 cycle of 1 min of pre-cooling, 6 min of run time, and 1 min of cooling time, 15 counts per second). Milled spores, defatted spores (9 mg/mL), and SpECs (94 mg/mL) were suspended in phosphate-buffered saline and stirred for 24 h at 4 °C. The suspension was then centrifuged at 2490 g for 10 min at 4 °C (Heraeus Multifuge X3R, Thermo Scientific, USA), and the supernatant was centrifuged again at 10621 g for 5 min at 4 °C (Eppendorf Centrifuge 5430R, Germany). The supernatant was used for protein profile analysis. For SDS-PAGE experiments, 8  $\mu$ L of each supernatant was mixed with 5  $\mu$ L NuPAGE® LDS sample buffer (4  $\times$  concentrated) (Invitrogen Life Technologies, Carlsbad, Calif., USA), 2  $\mu$ L NuPAGE® reducing agent, and 5  $\mu$ L MilliQ water. After centrifugation (1 min, 500 g, 20 °C), the solutions were heated for 10 min at 70 °C and centrifuged again (1 min, 500 g, 20 °C). From each sample, 10  $\mu$ L was loaded into individual lanes of a NuPAGE® 12% Bis-Tris Protein Gel, 1.0 mm, and run at 120 V (constant) with NuPAGE® 1x MES SDS running buffer. A protein molecular weight marker (5  $\mu$ L) was added in the first lane of the gel. The gel was stained with Colloidal Blue (G-250) (Thermo Fisher Scientific Inc.) for 3 h at 20 °C under slow shaking and later washed with deionized water while being shaken overnight.

### 2.3.3. Morphology of SpECs

The shape and morphological features of the spores and SpECs were imaged by scanning electron microscopy (SEM). Samples were fixated on aluminum sample stubs (9.5 mm) using carbon adhesive tabs. Before imaging, the samples were coated with gold by a sputter-coater (Smart-Coater, Joel Ltd., Akishima Tokyo, Japan). SEM images were taken at 5 kV, using a JEOL JCM-7000 (JEOL, Peabody, MA, USA).

## 2.4. Preparation of PEG and Dex stock solutions

Stock solutions of PEG (20 wt%) and Dex (10 wt%) were prepared in phosphate buffer (0.1 M) at pH values of 2, 4, and 7, at 20 °C. Solutions were stirred for 8 h to ensure complete hydration of the ingredients. Similarly, stock solutions of Dex (10 wt%) supplemented with a low concentration (0.075 wt%) of FITC-labeled Dex were prepared. According to the supplier (Sigma-Aldrich), the number of substituent molecules per glycosyl molecule in the polysaccharide chain of FITC-dextran ranged from 0.002 to 0.008. This indicates minimal alterations in charge and composition of the dextran. Sodium azide (0.5 mg/mL) was used to prevent microbial growth. Solutions were stored in the dark at 20 °C.

## 2.5. SpEC-free PEG-Dex all-aqueous systems

### 2.5.1. Microscopic imaging

Mixed solutions of the polymers were prepared by mixing PEG and Dex (supplemented with FITC-labeled Dex) stock solutions at different weight ratios of 1:9, 2:8, 3:7, 4:6, 5:5, 6:4, 7:3, 8:2, 9:1, which correspond to PEG: Dex concentration ratios of 2:9, 4:8, 6:7, 8:6, 10:5, 12:4, 14:3, 16:2, 18:1, respectively. The samples were microscopically imaged to determine the type of the all-aqueous emulsions, i.e., PEG-in-Dex or Dex-in-PEG. Immediately after mixing, a drop of each sample was placed on concave microscope glass slides, sealed with coverslips, and imaged by a Leica Confocal Laser Scanning Microscope (CLSM, TCS SP5, Leica Microsystems Inc., Germany). The excitation and emission wavelengths of the FITC-labeled Dex were 485 nm and 525, respectively.

### 2.5.2. Phase separation

The mixed bi-polymer solutions prepared at different concentration ratios of PEG: Dex (supplemented with FITC-labeled Dex) were allowed to phase separate for 24 h at 20 °C and then were imaged by a digital camera (Fujifilm, X-A3, Japan). The height of the top (PEG-rich) and bottom (Dex-rich) phases was measured using the software ImageJ and used for the approximation of the volume fraction of PEG ( $\varphi_{\text{PEG}}$ ) and Dex ( $\varphi_{\text{Dex}}$ ) phases.

## 2.6. SpEC-supplemented PEG-Dex all-aqueous systems

### 2.6.1. Supplementation with SpECs

Briefly, 50 mg of SpECs was suspended at the PEG stock solution at pH 7 and stirred (200 RPM) for 24 h. Then, the pairing solution, i.e., Dex (10 wt%) stock solution at pH 7 was added and the mixture was vortexed for 1 min at 200 RPM. The SpECs final concentration was 5 mg/mL. Samples were prepared in capped flat-bottomed cylindrical glass vials (22 mm × 66 mm).

Furthermore, mixed solutions of polymers at a PEG: Dex concentration ratio of 8:6 were prepared at pHs 2 and 4. Also, at a concentration ratio of 8:6 and pH 7, mixtures were prepared by initially suspending SpECs in the Dex solution as an alternative to initially suspending SpECs in the PEG solution.

To investigate the possible adsorption/absorption of Dex onto/into the particles, SpECs were suspended (5 mg/mL) in the Dex solution (10 wt%) supplemented with FITC-labeled Dex; then, the suspension was centrifuged, and the pellet was resuspended in Milli-Q water. The pellet was alternatively resuspended in the PEG solution (20 wt%) to assess whether PEG could de-wet the SpECs initially suspended in Dex. The

particles resuspended in PEG were subsequently centrifuged and resuspended in water before imaging by microscopy.

### 2.6.2. Microscopic imaging

The mixed systems of the polymers supplemented with SpECs were microscopically imaged after preparation. Immediately after mixing, a drop of each sample was placed in a concave microscope glass slide, sealed with a coverslip, and images were taken by a Leica Confocal Laser Scanning Microscope (CLSM, TCS SP5, Leica Microsystems Inc., Germany) as described before. Also, SpECs with FITC-labeled Dex were imaged by CLSM.

For phase contrast microscopy imaging, the samples were allowed to phase separate within the glass slides for 24 h. The time was long enough to reach a steady state so that the emulsion droplets no longer underwent coalescence. The images were taken with an Axioskop 50 light microscope, equipped with an AxioCam color camera (Carl Zeiss, Germany). Images were used to calculate the average diameter of emulsion droplets by image analysis software (Image J, NIH, Bethesda, MD, USA).

### 2.6.3. Phase separation and emulsification index

Mixed solutions of the polymers were prepared by mixing SpEC-supplemented PEG and FITC-Dex-supplemented Dex stock solutions at different weight ratios of PEG-to-Dex stock solutions between 1:9 and 9:1, corresponding to PEG: Dex concentration ratios between 2:9 and 18:1. The samples were allowed to phase separate in glass vials at 20 °C. The vials were then photographed after 24 h by a digital camera (Fujifilm, X-A3, Japan). The emulsification index (EI) and normalized emulsification index (NEI) of the samples were calculated as follows:

$$EI (\%) = \left( \frac{EH}{TH} \right) \times 100 \quad (1)$$

$$NEI (1 / g) = \left( \frac{EI}{Dex} \right) \times 100 \quad (2)$$

where EH and TH are the emulsion phase height and the total height of the sample, respectively, and Dex is the weight (g) of the Dex stock solution used in sample preparation. The sample prepared at the concentration ratio of 8:6 and pH 7 was selected to measure the emulsion index over time using equation (1).

### 2.6.4. Multiphoton excitation microscopy of SpECs at the interface

The emulsions prepared at the PEG: Dex concentration ratio of 8:6 and different pH values (2, 4, and 7), supplemented with SpECs, were imaged by multiphoton excitation microscopy (MPM, Leica SP8-Dive, Germany). Immediately after preparation a sample of each emulsion (200  $\mu$ L) was placed in an 8-well slide (Ibidi, GmbH, Martinsried, Germany) and analyzed after 10 min. An excitation wavelength of 800 nm, and an emission wavelength of 499–551 nm were used. Fluorescence Lifetime Imaging (FLIM) images were acquired at an area of 512 × 512 pixels, using a pixel dwell time of 1.7  $\mu$ s.

## 3. Results and discussion

### 3.1. Characterization of SpECs

The extracted SpECs had a mean particle size of ~31  $\mu$ m, which was slightly smaller than that of the parent spores (Table 1). The decrease in particle size was most likely due to the reduced hydration resulting from

**Table 1**  
Nitrogen content and particle size of *Lycopodium clavatum* spores and SpECs.

| Sample                    | Nitrogen (wt%) | Size ( $\mu$ m) |
|---------------------------|----------------|-----------------|
| <i>L. clavatum</i> spores | 1.25 ± 0.02    | 33.1 ± 0.2      |
| SpECs                     | 0.12 ± 0.04    | 31.1 ± 0.5      |

the removal of cytoplasmic material (Deng et al., 2019; Mundargi, Potroz, Park, Seo, Lee, et al., 2016). The protein content of the SpECs was significantly lower compared to that of the parent spores (Table 1), indicating that the extraction process efficiently removed most of the biological substances from the spores.

The electrophoretic pattern of the spores and defatted spores had an intense band at ~12 kDa and less intense bands at ~22 kDa to ~170 kDa (see Supplementary Fig. 1). The intense band of low molecular weight (i. e., ~12 kDa) has been already reported for *Lycopodium clavatum* spores (Uddin, Abidi, Warzywoda, & Gill, 2019) and was related to the proteins that are less tightly bound to the exines (Chay, Buehler, Thorn, Whelan, & Bedinger, 1992). The bands corresponding to larger proteins were not previously reported, possibly because we used a more sensitive stain (Colloidal Blue G-250) for protein bands detection compared to the preceding reports. In contrast to the spores, the SpECs did not have any detectable protein bands (Supplementary Fig. 1). We conclude that the SpECs were protein-free, and the small amount of nitrogen measured by the DUMAS method (Table 1) was attributable to nitrogen-containing compounds in the exine part of the spores (Uddin & Gill, 2018).

The *Lycopodium* spores and SpECs were examined by SEM and the images are shown in Fig. 1. Spores (Fig. 1 a and b) and SpECs (Fig. 1 c and d) both had a side with a lumen and murus seen as web-like microridges, and a tripartite structure (trilete) on the other side (Mundargi, Potroz, Park, Seo, Tan, et al., 2016). Even though the extraction process of SpECs caused slight changes in the trilete mark of the spores (Fig. 1 d), the obtained SpECs were mostly intact. When the SpECs were manually cracked (Fig. 1 e), they were hollow as expected.

Based on the results, the one-pot extraction protocol (Thomasson et al., 2020) applied in the current study removed all (or very most) of the proteins (some of them potentially allergenic) from *Lycopodium* spores while preserving their integrity and microstructure. The method saves time and money compared with conventional methods (Deng et al., 2019; Uddin & Gill, 2018). Next, all-aqueous emulsions of PEG and Dex were prepared, and the extracted SpECs were assessed for their potential as stabilizers of the emulsions.

### 3.2. SpEC-free PEG-Dex all-aqueous systems

Mixtures of PEG and Dex were prepared by mixing PEG (20 wt%) and Dex (10 wt%) stock solutions at different weight ratios of 1:9, 2:8, 3:7, 4:6, 5:5, 6:4, 7:3, 8:2, 9:1, which correspond to PEG: Dex concentration ratios between 2:9 to 18:1. The phase separation of two water-soluble and thermodynamically incompatible polymers at a moderately concentrated solution causes formation of all-aqueous emulsions. The phase diagram illustrated in Fig. 2, including the representative tie-lines, which were adopted from literature (Albertsson, 1986). The binodal (solid black line) in the phase diagram shows the transition from the single-phase region to the two-phase region. The extremum point on the curve where the tie lines get extremely short is referred to as the critical point. Towards the critical point the interfacial tension goes to zero and away from the point it becomes larger. Consistent with the expectation, the PEG-Dex mixtures in the two-phase region (indicated by the black

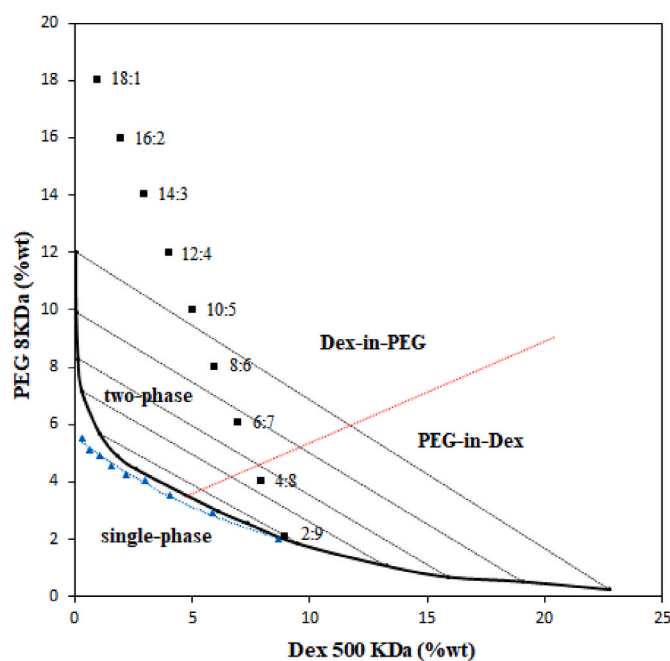


Fig. 2. Phase diagram of mixtures of polyethylene glycol (PEG, 20 wt%, 8 kDa) and dextran (Dex, 10 wt%, 500 kDa) [Adopted from Albertsson, 1986]. The filled squares represent the PEG: Dex concentration ratios in the mixtures at the present study. The tie lines and the binodal (from Albertsson, 1986) are indicated by discontinued black lines, and by the solid black line, respectively. The approximated phase inversion from Dex-continuous to PEG-continuous two-phase systems, which occurs in the center of the tie-lines, is denoted by the red line. Blue triangles depict our data collection, and the discontinued blue line represents the fitted line to the data.

squares in Fig. 2) phase separated into two distinct phases once they were allowed to rest (i.e., no mixing).

At the PEG: Dex concentration ratios of 2:9 and 4:8; CLSM imaging (Supplementary Fig. 2) indicated that the emulsions were Dex-continuous, whereas the emulsions were PEG-continuous when the ratio was 6:7 and higher. In the phase diagram (Fig. 2), the blue triangles represent our data collection, with the fitted line to the data. Our data and the fitted line are in agreement with those obtained from the literature (Albertsson, 1986). The red line represents the center of the tie-lines, where the volume ratio of the bi-polymer mixture is 50:50 and the phase inversion takes place (Albertsson, 1986). The approximated phase inversion (red line in Fig. 2) corresponds to the observed transition from Dex-continuous (PEG-in-Dex) to PEG-continuous (Dex-in-PEG) emulsions once the concentration ratio changed from 4:8 to 6:7. The volume ratio of the polymer phases after the mixtures phase separation was measured at different concentration ratios. Supplementary Fig. 3 shows photographs of the phase-separated emulsions with the top PEG-rich and bottom Dex-rich phases. The bottom Dex phase was green because it included FITC-labeled Dex. Approximation of the volume

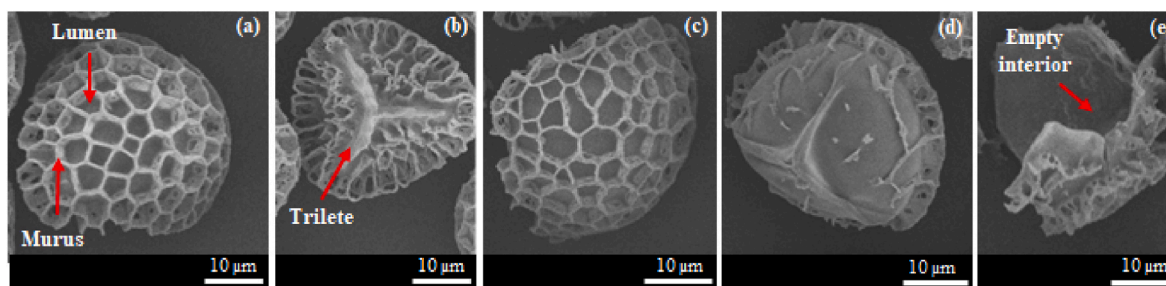


Fig. 1. SEM micrographs of (a) and (b) *Lycopodium clavatum* spores; (c) and (d) sporopollenin exine capsules (SpECs); and (e) manually cracked SpECs.

fraction of the top ( $\varphi_{\text{PEG}}$ ) and bottom ( $\varphi_{\text{Dex}}$ ) phases indicated that the transition from a PEG-in-Dex to a Dex-in-PEG emulsion took place when  $\varphi_{\text{PEG}}$  roughly exceeded 0.43 (red line in Sup. Fig. 3). The observed transition at  $\varphi_{\text{PEG}}$  between 0.43 and 0.6 coincides with the theoretical phase inversion of systems without added stabilizer particles at a volume ratio of 0.5, i.e., approximate equality in the volume fraction of the two phases (Esquena, 2016).

### 3.3. Stabilization of all-aqueous emulsion by SpECs

SpECs were assessed for their efficacy to stabilize the all-aqueous emulsions prepared at different concentration ratios of PEG: Dex at pH 7 (represented by the black filled squares in Fig. 2). Fig. 3 shows the photographs of samples after 24 h resting. In Dex-continuous two-phase systems, i.e., at the concentration ratios  $\leq 4:8$ , as well as at the ratio of 6:7 (the transitional ratio from Dex-continuous to PEG-continuous emulsion), samples phase separated into a top PEG-rich and a bottom Dex-rich phases, and the SpECs agglomerated at the water-water interface between the phases. However, at the concentration ratios of 8:6 and higher, a bottom emulsion phase in co-existence with a top PEG phase was observed. The observations implied that the SpECs could stabilize PEG-continuous emulsions (concentration ratios  $\geq 8:6$ ) but not the Dex-continuous (concentration ratios  $\leq 4:8$ ) counterparts.

The samples that yielded a stable emulsion phase (concentration ratios  $\geq 8:6$ ) were prepared again and this time were allowed to rest in the wells of a microscope slide so that the bottom emulsion phase could be imaged *in situ* by CLSM and optical microscopy (Fig. 4). Confocal images confirmed that the emulsion phase was PEG-continuous (i.e., Dex-in-PEG). Moreover, the optical microscopy (inserts in Fig. 3) and CLSM images (Fig. 4) indicated that SpECs adsorbed at the surface of dispersed phase droplets. The accumulation of SpECs at the water-water interface between the Dex and PEG phases can be ascribed to a Pickering-type mechanism. Once present at the interface, the particles can pack at different configurations, depending on repulsive electrostatic interactions and attractive capillary-driven interactions. The capillary interactions have been shown to form particle rafts in oil-water interfaces, which can be either densely or loosely packed (Protière, 2023) and may arise from a large size, a rough particle shape, and a high density of the particles (Binks, Boa, Kibble, MacKenzie, & Rocher, 2011; Kralchevsky, Denkov, & Danov, 2001). The SpECs have a higher density, a value most probably lying between 1.65 and 1.96 g/cm<sup>-3</sup> (Cojocaru et al., 2022), than the density of the two liquid phases, most likely ranging between 1.03 and 1.06 (Bosek et al., 2022; Fischer, 2010;

González-Tello, Camacho, & Blázquez, 1994). Although the water-water interface is more diffuse than an oil-water interface, a similar packing mechanism may also occur in all-aqueous emulsions that could contribute to emulsion stability. In addition, some of the SpECs could also be present in the continuous phase, which may limit coalescence of the dispersed droplet, due to physical hindrance. It is worth noting that even though some SpECs were broken (i.e., red circle in Fig. 4, ratio 8:6), these were scarce and were not expected to significantly impact the emulsion stability.

Droplet size measurements (Table 2) indicated that the higher the PEG: Dex concentration ratio the smaller the emulsion droplets, i.e., the emulsion droplet size decreased as the concentration of SpECs relative to the dispersed Dex phase increased. This is in line with the observations for oil-water emulsions stabilized by SpEC particles, for which the stability to both creaming and coalescence increased with particle concentration due to a progressive decrease in droplet size (Binks et al., 2011). In the current study, the SpECs were large ( $\sim 31 \mu\text{m}$ ), and their high density led to sedimentation of the droplets to the bottom of the container, although the droplets itself were stabilized against coalescence. One could alternatively use SpECs extracted from other resources such as *Myosotis* (2.4–5  $\mu\text{m}$ ), *Chlorella vulgaris* (8–10  $\mu\text{m}$ ) and *Ambrosia trifida* (Ragweed) (15  $\mu\text{m}$ ) (Diego-Taboada et al., 2014) to possibly fabricate smaller emulsion droplets and improve stability against sedimentation.

In addition to EI, the normalized emulsification index (NEI), which expresses the EI relative to the proportion of the Dex phase in each emulsion is reported in Table 2. The EI decreased with increasing PEG: Dex concentration ratios in the emulsions. This indicates that the volume of the emulsion phase was mainly determined by the proportion of the Dex phase and that the emulsion phase was in equilibrium with an excess of the PEG phase. The NEI did not follow the same trend as the EI. The emulsions prepared at the PEG: Dex concentration ratios  $\leq 14:3$  had comparable NEIs but at the ratios of 16:2 and 18:1, the NEI increased with decreasing EI (Table 2). It was decided to continue the study by making samples at a concentration ratio of 8:6 because it provided the highest EI (making it easier to characterize the emulsion phase) and yet a comparable NEI with those of the samples at ratios up to 14:3 (Table 2).

The EI of the sample prepared at the concentration ratio of 8:6 decreased over a storage period of 96 h (Supplementary Fig. 4). During storage, the emulsion phase itself phase-separated into a lower Dex phase and an upper emulsion phase. The decrease in EI (Supplementary Fig. 4) is ascribed to Dex-rich droplet coalescence and the subsequent

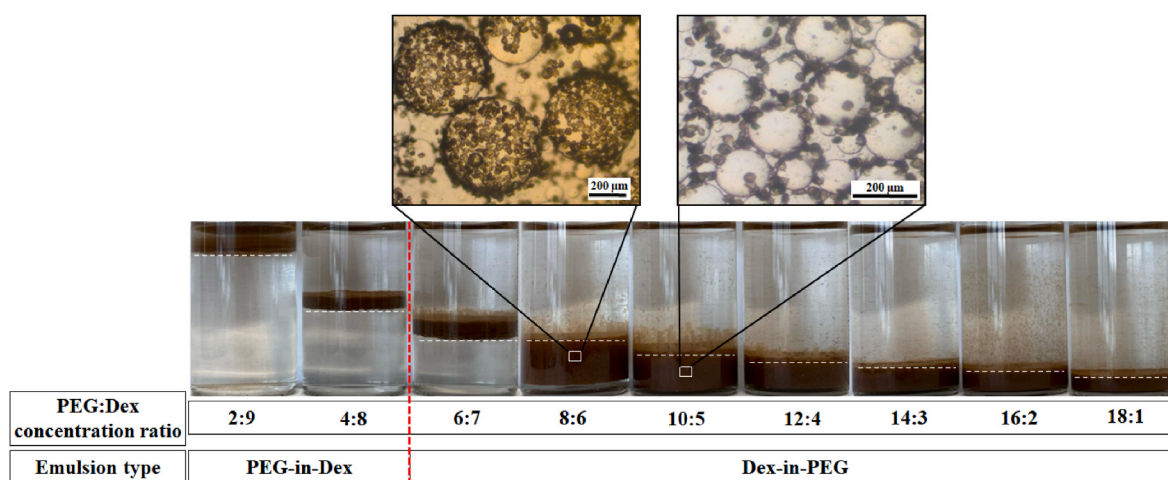
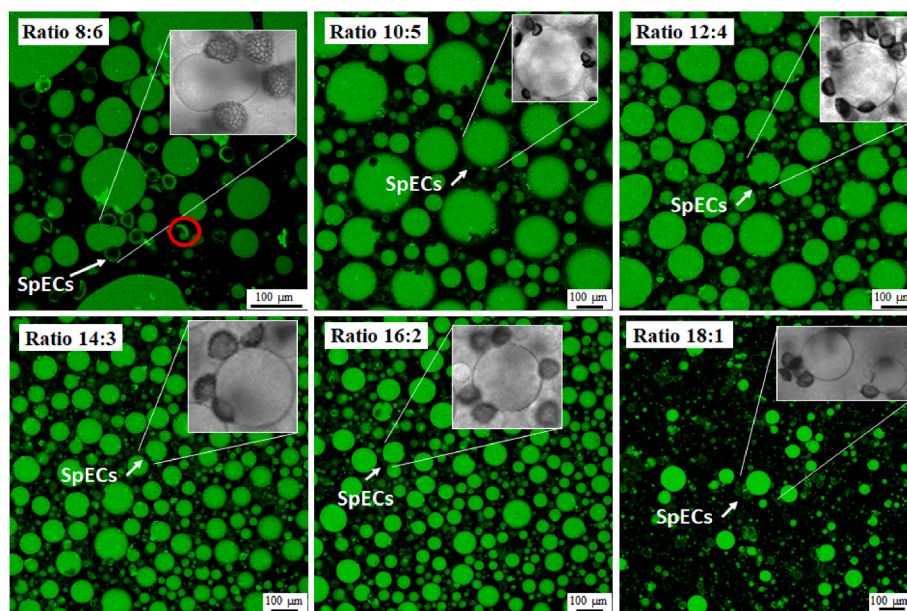


Fig. 3. Photographs of SpECs-supplemented all-aqueous emulsions of polyethylene glycol (PEG, 20 wt%, 8 kDa) and dextran (Dex, 10 wt%, 500 kDa) at all studied PEG: Dex concentration ratios. The images were taken 24 h after mixing the polymer phases. Dotted lines depict the interface between the two phases. The top phase always contained PEG, and the bottom phase was either a Dex phase (ratios  $\leq 6:7$ ) or an emulsion phase (ratios  $\geq 8:6$ ). The insets show the location of the SpECs at the water-water interface, imaged by a light microscope. The red line represents the phase inversion.



**Fig. 4.** CLSM micrographs of SpECs-supplemented all-aqueous emulsions (5 mg/mL) of polyethylene glycol (PEG, 20 wt%, 8 kDa) and dextran (Dex, 10 wt%, 500 kDa). The values are PEG: Dex concentration ratios in the emulsions. Green indicates the Dex phase (supplemented with FITC-labeled Dex), and black indicates the PEG phase. The insets show the location of the SpECs at the water-water interface, imaged by light microscopy.

**Table 2**

Droplet size, emulsification index (EI), and normalized emulsification index (NEI) of the emulsions at different PEG: Dex concentration ratios.

| Concentration ratio | Droplet size ( $\mu\text{m}$ ) | EI (%) | NEI (1/g) |
|---------------------|--------------------------------|--------|-----------|
| 8:6                 | $344 \pm 52$                   | 27.22  | 4.54      |
| 10:5                | $221 \pm 39$                   | 23.35  | 4.67      |
| 12:4                | $173 \pm 36$                   | 17.43  | 4.36      |
| 14:3                | $130 \pm 23$                   | 13.62  | 4.54      |
| 16:2                | $97 \pm 17$                    | 12.54  | 6.27      |
| 18:1                | $64 \pm 9$                     | 8.84   | 8.84      |

drainage of Dex from the emulsion phase. It has already been shown that Pickering-stabilized oil-in-water droplets can merge through a so-called multi-body coalescence mechanism, i.e., the simultaneous coalescence of multiple droplets in a single event (Wu et al., 2015). For oil-water interfaces with an interfacial tension in the order of 30 mN/m, a particle radius of 200 nm, and a contact angle of  $90^\circ$ , the desorption energy is  $9.2 \cdot 10^5$  kT. For all-aqueous emulsions, although the interfacial tension is of the order of 1  $\mu\text{N/m}$ , the large particle radius of SpECs (15  $\mu\text{m}$ ) causes a desorption energy only one order of magnitude lower,  $1.7 \cdot 10^5$  kT, for a similar contact angle. Hence, emulsion stability can be related to the large size of SpECs, and the high desorption energy confirms that the particles indeed provide Pickering stabilization. However, the lower adsorption/desorption energy of the stabilizer particles in all-aqueous emulsions may increase the likelihood of the particle desorption from the interface during the coalescence process. In addition, due to the large size, high gravitational forces would favor further sedimentation through removal from the interface. These events most likely explain the emulsion destruction and EI reduction (Table 2). The desorption of SpECs from the interface was confirmed by the adherence of the particles to the inner walls of the sample glass containers.

The stability of all-aqueous emulsions may vary depending on multiple factors including but not limited to stabilizer particle size, shape, and wettability (Dickinson, 2019; Guzmán et al., 2022) and the preparation procedure. The latter was studied by preparing emulsions (at a PEG: Dex ratio of 8:6) via initially dispersing the SpECs in the Dex phase instead of the PEG phase. When SpECs were initially dispersed in the Dex phase rather than the PEG phase, the bottom emulsion phase was less

stable and separated into a clear Dex phase within the first 24 h (Supplementary Fig. 5). The emulsion stability was thus dependent on the polymer phase in which the SpECs were initially dispersed. This observation is in agreement with our hypothesis that the SpECs in the continuous PEG phase could stabilize the emulsion further by limiting the likelihood of droplet coalescence. In addition, differences in wetting ability of the fluids may be responsible. The Dex solution was of higher viscosity ( $\sim 50$  mPa s) (Fischer, 2010) than the PEG solution ( $\sim 20$  mPa s) (González-Tello et al., 1994). One can assume that a fluid with a lower viscosity like the PEG solution would wet the particles more easily than the more viscous Dex solution and can therefore be included at the interface easier. In contrast, when the particles were initially introduced into the Dex solution, upon subsequent mixing of the solutions, PEG could not adequately de-wet the particles from Dex.

The efficacy of PEG to de-wet SpECs in subsequent to suspending in Dex was assessed. For this purpose, SpECs were suspended in FITC-labeled Dex and centrifuged. Then the pellet was resuspended in PEG solution prior to further centrifugation and resuspension in water before imaging by CLSM. *Lycopodium* spores exhibit fluorescence under multiple excitation wavelengths (Mundargi, Potroz, Park, Seo, Tan, et al., 2016). One channel includes excitation at 561 nm and emission at 595 nm, which is different from the excitation and emission wavelengths of FITC (for FITC-labeled Dex) at 485 nm and 525 nm, respectively. In Fig. 5, the green channel detects both the FITC-labeled Dex and the SpECs auto-fluorescence, and the purplish red (magenta) channel detects only the SpECs auto-fluorescence. The images of SpECs suspended in water show a hollow, not fluorescent interior. Therefore, the green fluorescence signal detected at the interior of the SpECs which were initially suspended in Dex, then centrifuged (to remove excess Dex) and resuspended in water indicates that SpECs were filled with Dex. The observation of the Dex signal also in the SpECs resuspended in PEG shows (and supports the abovementioned hypothesis) that PEG could not de-wet the particles once they were initially suspended in Dex. As the Dex used in the present study was of much larger molecular weight than the PEG, we assume that when SpECs were initially dispersed in the PEG solution prior to emulsification, PEG was also able to fill the interior of the particles. However, this assumption needs verification, taking into consideration the difference in the hydrophobicity of Dex and PEG.

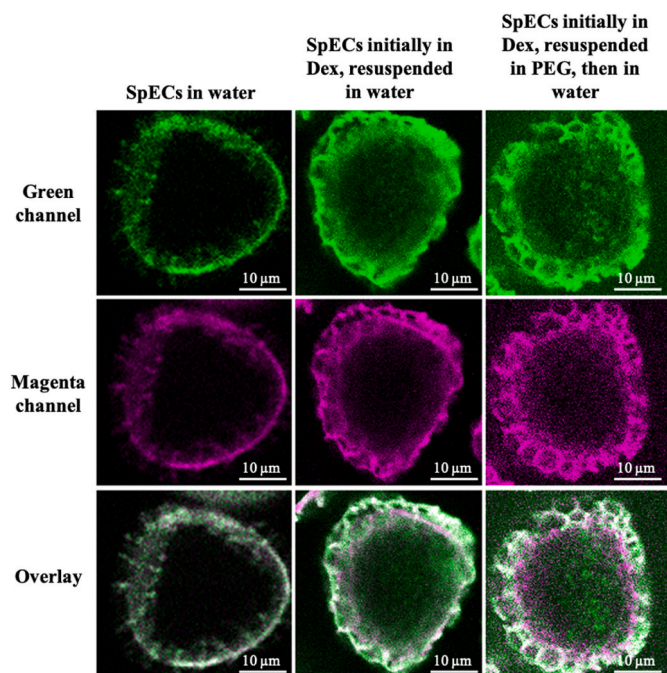


Fig. 5. CLSM micrographs of SpECs suspended in different media. Green indicates the auto-fluorescence of SpECs and the FITC-labeled Dex, and magenta indicates the SpECs auto-fluorescence.

### 3.4. Effect of pH on emulsion stability

The efficacy of SpECs in stabilizing all-aqueous emulsions might also depend on the emulsion pH value. Sporopollenin is a biopolymer with building blocks containing poly(hydroxy acid) groups (Mikhael et al., 2020). As pH increases, the number of ionized functional groups (e.g., the negatively charged carboxylic acid groups) on the surface of the SpECs will increase, which in turn, will increase the SpECs hydrophilicity (Chiappe et al., 2020; Mackenzie, Beckett, Atkin, & Diego-Taboada, 2014, 2015). To gain more insight into this, emulsion samples at a concentration ratio of 8:6 were prepared at different pH values of 2, 4, and 7, and the  $\zeta$ -potential of SpECs was measured as a function of pH between 2 and 7 (see Fig. 6).

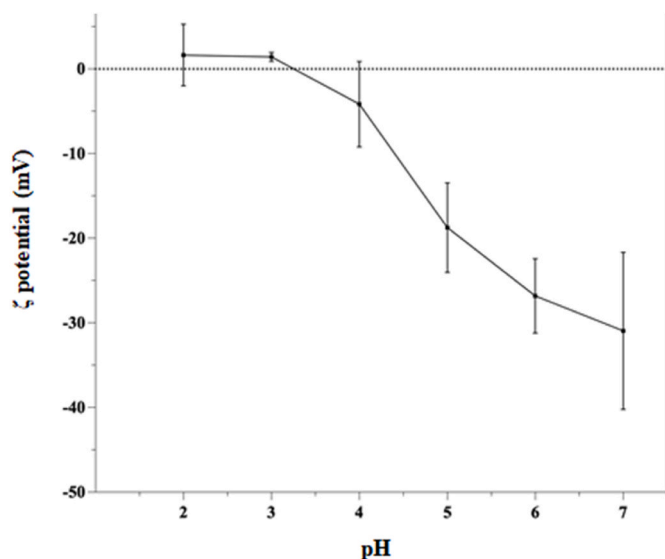


Fig. 6.  $\zeta$ -potential of sporopollenin exine capsules (SpECs) as a function of pH at 20 °C.

SpECs were strongly negatively charged at pH 7 and had a  $\zeta$ -potential value of about  $-31$  mV. The  $\zeta$ -potential of SpECs decreased with decreasing pH to 4 and became slightly positive at pH 2. The  $\zeta$ -potential results obtained in the present study are not in line with those reported by Binks et al. (2011). The differences may be attributed to variations in the extraction protocols employed in the two studies. In our study, a one-pot acidic treatment was applied, whereas Binks and coworkers applied an alkaline treatment in addition to an acid treatment (Binks et al., 2011). The use of different protocols may induce variability in the quantity of functional groups on the surface of the SpECs (Thomasson et al., 2020). These changes in the composition may influence the properties of the SpECs.

PEG and Dex are non-ionic polymers and changes in pH should hardly influence their incompatibility. Fig. 7 shows images of the emulsions formed at different pH values.

Fig. 7 shows that, among the samples at different pHs, only the emulsion at pH 7 remained stable after 24 h and Fig. 8 indicates that at pHs 2 and 4 the SpECs were positioned compactly at the water-water interface. In particular at pH 2, the SpECs formed quite a dense layer at the interface, whereas at pH 7, SpECs were positioned less compactly. The latter is ascribed to the interparticle repulsion between the SpECs at pH 7 due to the particles high  $\zeta$ -potential value (Fig. 6). In general, it is believed that a higher packing leads to more stable emulsions, due to a lower degree of coalescence and the possible formation of rafts due to capillary interactions (Protière, 2023). However, in the case of the SpEC-stabilized emulsions, a less packed interface due to increased electrostatic repulsion was more beneficial to provide stability. Overall, these results show that close particle packing at the interface is not the most important parameter, and that electrostatic repulsion between particles and dispersed droplets is more beneficial for emulsion stability. This would also support our hypothesis that particles present in the continuous phase can contribute to the stability of the emulsions.

## 4. Conclusion

The extraction protocol of sporopollenin exine capsules efficiently removed (glycol)proteins and cytoplasmic components from *Lycopodium clavatum* spores. These particles were shown to stabilize all-aqueous emulsions formed from mixtures of PEG and Dex, but only under certain conditions. Upon addition of the SpECs into the PEG phase and subsequent preparation of PEG-Dex two-phase systems, the SpECs adsorbed at the aqueous-aqueous interface, causing formation of stabilized Dex-rich droplets in a continuous PEG phase. The stability of the emulsion phase was attributed to a Pickering-type stabilization mechanism, possible formation of SpEC rafts at the interface, and the physical hindrance to droplets coalescence by the SpECs remained suspended in the continuous PEG phase. The emulsion phase stability was dependent on the pH value of the system. Although the emulsions were more stable

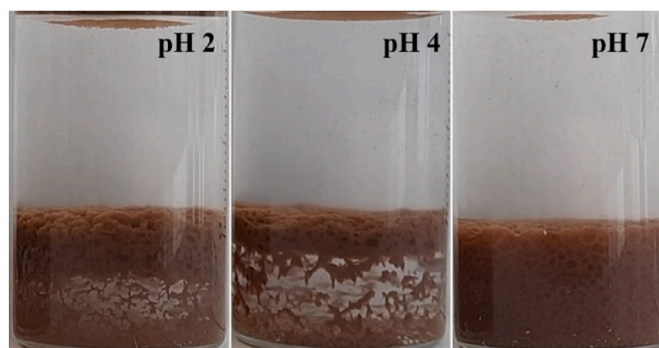
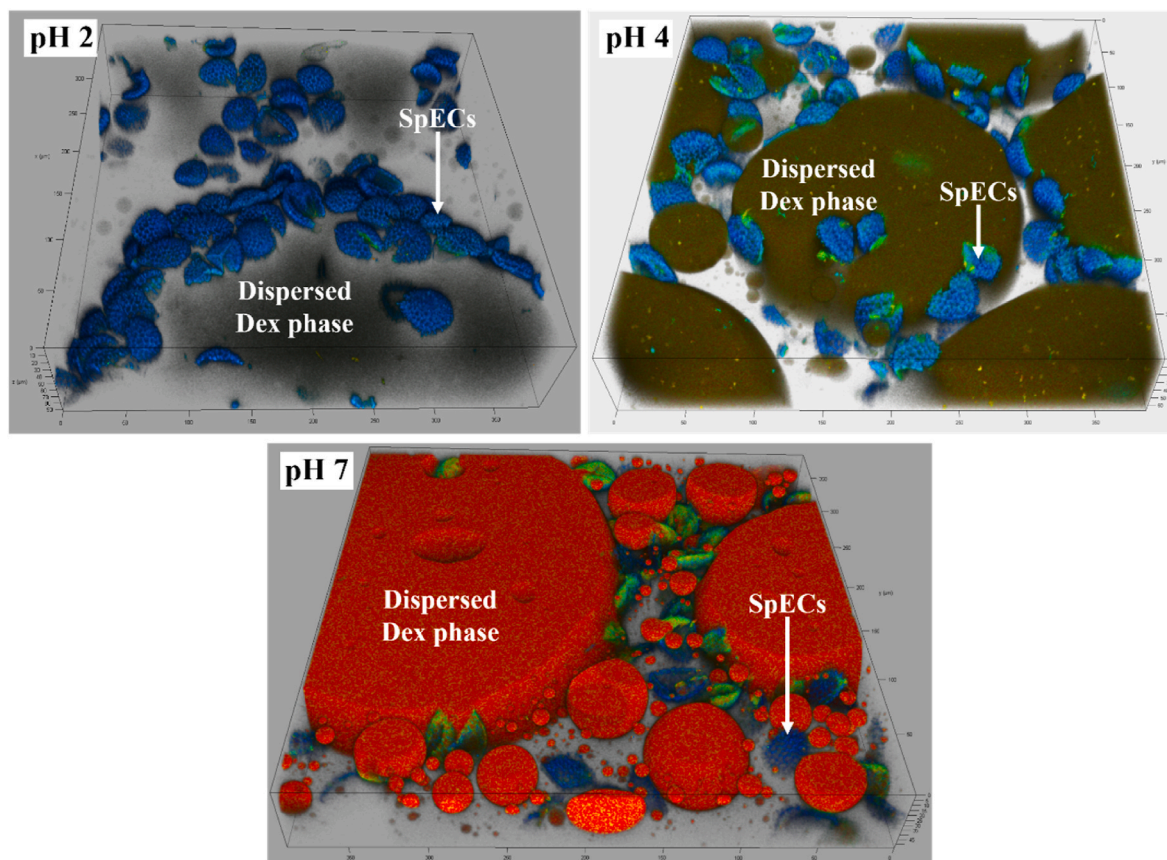


Fig. 7. Dex-in-PEG emulsions at a PEG: Dex concentration ratio of 8:6, and stabilized with SpECs (5 mg/mL) at different pHs; the images were taken 24 h after mixing the polymer phases.



**Fig. 8.** Two-photon confocal micrographs of Dex-in-PEG emulsions stabilized with SpECs (5 mg/mL) at a PEG: Dex concentration ratio of 8:6, at pH 2, pH 4, and pH 7. Blue indicates the autofluorescence of SpECs. Black (pH 2), green (pH 4), and orange (pH 7) indicate the Dex phase (supplemented with FITC-labeled Dex).

at pH 7, less particles were present at the interface, indicating that the repulsion between particles at this pH was more important than the particle packing density at the interface. Physical hindrance to droplet coalescence by negatively-charged particles in the continuous phase could also contribute to the stability. These results show that the naturally available SpECs show potential to be used in the design of emulsions based on water and hydrocolloids only. Emulsion stability may be further increased by the use of SpECs with smaller sizes.

#### CRediT author statement

Diana Soto-Aguilar: Investigation; Resources; Formal analysis; Writing-Original, Elke Scholten, Conceptualization; Supervision; Validation; Writing-Review & Editing., Vincenzo Fogliano: Conceptualization; Supervision; Writing-Review & Editing; Project administration., Ashkan Madadlou: Conceptualization; Methodology; Writing-Review & Editing; Supervision.

#### Declaration of competing interest

The authors declare that they have no known competing financial interests or personal relationships that could have appeared to influence the work reported in this paper.

#### Data availability

Data will be made available on request.

#### Acknowledgments

We gratefully acknowledge the financial support from CONACYT

(grant number 739555).

#### Appendix A. Supplementary data

Supplementary data to this article can be found online at <https://doi.org/10.1016/j.foodhyd.2023.109447>.

#### References

- Abkarian, M., Protière, S., Aristoff, J. M., & Stone, H. A. (2013). Gravity-induced encapsulation of liquids by destabilization of granular rafts. *Nature Communications*, 4. <https://doi.org/10.1038/ncomms2869>
- Albertsson, P. A. (1986). *Partition of cell particles and macromolecules: Separation and purification of biomolecules, cell organelles, membranes, and cells in aqueous polymer two-phase systems and their use in biochemical analysis and biotechnology* (3rd ed.). Wiley. <https://doi.org/10.1002/cbf.290050311>
- Bailey, C. S., Zarins-Tutt, J. S., Agbo, M., Gao, H., Diego-Taboada, A., Gan, M., et al. (2019). A natural solution to photoprotection and isolation of the potent polyene antibiotic, marinomycin A. *Chemical Science*, 10(32), 7549–7553. <https://doi.org/10.1039/c9sc01375j>
- Barrier, S. (2008). *Physical and chemical properties of sporopollenin exine particles [Thesis dissertation]*. <https://hydra.hull.ac.uk/resources/hull:6412>
- Binks, B. P., Boa, A. N., Kibble, M. A., MacKenzie, G., & Rocher, A. (2011). Sporopollenin capsules at fluid interfaces: Particle-stabilised emulsions and liquid marbles. *Soft Matter*, 7(8), 4017–4024. <https://doi.org/10.1039/c0sm01516d>
- Binks, B. P., Clint, J. H., Mackenzie, G., Simcock, C., & Whitby, C. P. (2005). Naturally occurring spore particles at planar fluid interfaces and in emulsions. *Langmuir*, 21(18), 8161–8167. <https://doi.org/10.1021/la0513858>
- Bosek, M., Ziolkowska, B., Pyskir, J., Wybranowski, T., Pyskir, M., Cyrankiewicz, M., et al. (2022). Relationship between red blood cell aggregation and dextran molecular mass. *Scientific Reports*, 12(1). <https://doi.org/10.1038/s41598-022-24166-w>
- Chay, C. H., Buehler, E. G., Thorn, J. M., Whelan, T. M., & Bedinger, P. A. (1992). Purification of maize pollen exines and analysis of associated proteins. *Plant Physiology*, 100. <https://academic.oup.com/plphys/article/100/2/756/6085911>
- Chen, J. F., Guo, J., Liu, S. H., Luo, W. Q., Wang, J. M., & Yang, X. Q. (2019). Zein particle-stabilized water-in-water emulsion as a vehicle for hydrophilic bioactive compound loading of Riboflavin. *Journal of Agricultural and Food Chemistry*, 67(35), 9926–9933. <https://doi.org/10.1021/acs.jafc.9b02415>



- Chiappe, C., Rodriguez-Douton, M. J., Mozzati, M. C., Prete, D., Griesi, A., Guazzelli, L., et al. (2020). Fe-Functionalized paramagnetic sporopollenin from pollen grains: One-pot synthesis using ionic liquids. *Scientific Reports*, 10(1), 1–11. <https://doi.org/10.1038/s41598-020-68875-6>
- Cojocar, R., Mannix, O., Capron, M., Giles Miller, C., Jouneau, P.-H., Gallet, B., et al. (2022). A biological nanofoam: The wall of coniferous bisaccate pollen. *Science Advances*, 8.
- Dahl, Å. (2018). Pollen lipids can play a role in allergic airway inflammation. *Frontiers in Immunology*, 9, 2816. <https://doi.org/10.3389/fimmu.2018.02816>. NLM (Medline).
- Deng, Z., Pei, Y., Wang, S., Zhou, B., Li, J., Hou, X., et al. (2019). Carboxymethylpachymaran entrapped plant-based hollow microcapsules for delivery and stabilization of  $\beta$ -galactosidase. *Food & Function*, 10(8), 4782–4791. <https://doi.org/10.1039/c9fo00649d>
- Dickinson, E. (2019). Particle-based stabilization of water-in-water emulsions containing mixed biopolymers. *Trends in Food Science and Technology*, 83, 31–40. <https://doi.org/10.1016/j.tifs.2018.11.004>. Elsevier Ltd.
- Diego-Taboada, A., Beckett, S. T., Atkin, S. L., & Mackenzie, G. (2014). Hollow pollen shells to enhance drug delivery. *Pharmaceutics*, 6(1), 80–96. <https://doi.org/10.3390/pharmaceutics6010080>
- Esquena, J. (2016). Water-in-water (W/W) emulsions. *Current Opinion in Colloid & Interface Science*, 25, 109–119. <https://doi.org/10.1016/j.cocis.2016.09.010>. Elsevier Ltd.
- Fischer, T. M. (2010). A method to prepare isotonic dextran - salt solutions. *Cytometry, Part A*, 77(8), 805–810. <https://doi.org/10.1002/cyto.a.20909>
- Gonçalves, R. F. S., Martins, J. T., Duarte, C. M. M., Vicente, A. A., & Pinheiro, A. C. (2018). Advances in nutraceutical delivery systems: From formulation design for bioavailability enhancement to efficacy and safety evaluation. *Trends in Food Science and Technology*, 78, 270–291. <https://doi.org/10.1016/j.tifs.2018.06.011>. Elsevier Ltd.
- González-Tello, P., Camacho, F., & Blázquez, G. (1994). Density and viscosity of concentrated aqueous solutions of polyethylene glycol. *Journal of Chemical and Engineering Data*, 39(3), 611–614. <https://doi.org/10.1021/je00015a050>
- Guzmán, E., Martínez-Pedrero, F., Calero, C., Maestro, A., Ortega, F., & Rubio, R. G. (2022). A broad perspective to particle-laden fluid interfaces systems: From chemically homogeneous particles to active colloids. *Advances in Colloid and Interface Science*, 302. <https://doi.org/10.1016/j.cis.2022.102620>. Elsevier B.V.
- Hazt, B., Bassani, H. P., Elias-Machado, J. P., Buzzo, J. L. A., Silveira, J. L., & de Freitas, R. A. (2020). Effect of pH and protein particle shape on the stability of amylopectin – xyloglucan water-in-water emulsions (Vol. 104), Article 105769. <https://doi.org/10.1016/j.foodhyd.2020.105769>
- Kralchevsky, P. A., Denkov, N. D., & Danov, K. D. (2001). Particles with an undulated contact line at a fluid interface: Interaction between capillary quadrupoles and rheology of particulate monolayers. *Langmuir*, 17(24), 7694–7705. <https://doi.org/10.1021/la0109359>
- Lagubeau, G., Rescaglio, A., & Melo, F. (2014). Armoring a droplet: Soft jamming of a dense granular interface. *Physical Review E - Statistical, Nonlinear and Soft Matter Physics*, 90(3). <https://doi.org/10.1103/PhysRevE.90.030201>
- Mackenzie, G., Beckett, S., Atkin, S., & Diego-Taboada, A. (2014). Pollen and spore shells—nature’s microcapsules. In *Microencapsulation in the food industry: A practical implementation guide* (pp. 283–297). Elsevier. <https://doi.org/10.1016/B978-0-12-404568-2.00024-8>.
- Mackenzie, G., Boa, A. N., Diego-Taboada, A., Atkin, S. L., & Sathyapalan, T. (2015). Sporopollenin, the least known yet toughest natural biopolymer. *Frontiers in Materials*, 2, 66. <https://doi.org/10.3389/fmats.2015.00066>. Frontiers Media S.A.
- Madadlou, A., Saggiomo, V., Schroën, K., & Fogliano, V. (2020). All-aqueous emulsions as miniaturized chemical reactors in the food and bioprocess technology. *Current Opinion in Food Science*, 33, 165–172. <https://doi.org/10.1016/j.cofs.2020.06.005>
- McClements, D. J. (2020). Advances in nanoparticle and microparticle delivery systems for increasing the dispersibility, stability, and bioactivity of phytochemicals. *Biotechnology Advances*, 38, Article 107287. <https://doi.org/10.1016/j.biotechadv.2018.08.004>. July 2018.
- Mikhael, A., Jurcik, K., Schneider, C., Karr, D., Fisher, G. L., Fridgen, T. D., et al. (2020). Demystifying and unravelling the molecular structure of the biopolymer sporopollenin. *Rapid Communications in Mass Spectrometry*, 34(10). <https://doi.org/10.1002/rcm.8740>
- Mundargi, R. C., Potroz, M. G., Park, J. H., Seo, J., Lee, J. H., & Cho, N. J. (2016). Extraction of sporopollenin exine capsules from sunflower pollen grains. *RSC Advances*, 6(20), 16533–16539. <https://doi.org/10.1039/c5ra27207f>
- Mundargi, R. C., Potroz, M. G., Park, J. H., Seo, J., Tan, E. L., Lee, J. H., et al. (2016). Eco-friendly streamlined process for sporopollenin exine capsule extraction. *Scientific Reports*, 6. <https://doi.org/10.1038/srep19960>
- Nicolai, T., & Murray, B. (2017). Particle stabilized water in water emulsions. *Food Hydrocolloids*, 68, 157–163. <https://doi.org/10.1016/j.foodhyd.2016.08.036>
- Protière, S. (2023). Particle rafts and armored droplets. *Annual Review of Fluid Mechanics*, 55, 459–480. <https://doi.org/10.1146/annurev-fluid-030322>
- Scholten, E., Sagis, L. M. C., & Van Linden, E. Der (2006). Effect of bending rigidity and interfacial permeability on the dynamical behavior of water-in-water emulsions. *Journal of Physical Chemistry B*, 110(7), 3250–3256. <https://doi.org/10.1021/jp056528d>
- Schouten, P. J., Soto-Aguilar, D., Aldabahi, A., Ahamad, T., Alzahly, S., & Fogliano, V. (2022). Design of sporopollenin-based functional ingredients for gastrointestinal tract targeted delivery. *Current Opinion in Food Science*, 44, Article 100809. <https://doi.org/10.1016/j.cofs.2022.100809>
- Tea, L., Renou, F., & Nicolai, T. (2021). Effect of hydrophobicity and molar mass on the capacity of chitosan and  $\kappa$ -carrageenan to stabilize water in water emulsions. *Carbohydrate Polymers*, 271(July), Article 118423. <https://doi.org/10.1016/j.carbpol.2021.118423>
- Thomasson, M. J., Diego-Taboada, A., Barrier, S., Martin-Guyout, J., Amedjou, E., Atkin, S. L., et al. (2020). Sporopollenin exine capsules (SpECs) derived from *Lycopodium clavatum* provide practical antioxidant properties by retarding rancidification of an  $\omega$ -3 oil. *Industrial Crops and Products*, 154(June), Article 112714. <https://doi.org/10.1016/j.indcrop.2020.112714>
- Troise, A. D., Fogliano, V., & Madadlou, A. (2020). Tailor it up! How we are rolling towards designing the functionality of emulsions in the mouth and gastrointestinal tract. *Current Opinion in Food Science*, 31, 126–135. <https://doi.org/10.1016/j.cofs.2020.06.002>. Elsevier Ltd.
- Uddin, M. J., Abidi, N., Warzywoda, J., & Gill, H. S. (2019). Investigation of the fate of proteins and hydrophilicity/hydrophobicity of *Lycopodium clavatum* spores after organic solvent-base-acid treatment. *ACS Applied Materials and Interfaces*, 11(23), 20628–20641. <https://doi.org/10.1021/acsami.9b03040>
- Uddin, M. J., & Gill, H. S. (2018). From allergen to oral vaccine carrier: A new face of ragweed pollen. *International Journal of Pharmaceutics*, 545(1–2), 286–294. <https://doi.org/10.1016/j.ijpharm.2018.05.003>